

Ultrahigh finesse Fabry-Perot superconducting resonator

S. Kuhr, S. Gleyzes, C. Guerlin, J. Bernu, U. B. Hoff, S. Deléglise, S. Osnaghi, M. Brune, and J.-M. Raimond
*Laboratoire Kastler Brossel, Département de Physique de l'École Normale Supérieure,
24 rue Lhomond, F-75231 Paris Cedex 05, France*

S. Haroche
Collège de France, 11 Place Marcelin Berthelot, F-75231 Paris Cedex 05, France

E. Jacques, P. Bosland, and B. Visentin
DAPNIA, Orme des Merisiers, CEA, F-91191 Gif-sur-Yvette Cedex, France
(Dated: November 26, 2024)

We have built a microwave Fabry-Perot resonator made of diamond-machined copper mirrors coated with superconducting niobium. Its damping time ($T_c = 130$ ms at 51 GHz and 0.8 K) corresponds to a finesse of 4.6×10^9 , the highest ever reached for a Fabry-Perot in any frequency range. This result opens many perspectives for quantum information processing, decoherence and non-locality studies.

PACS numbers: 42.50.Pq, 03.67.-a, 84.40.-x, 85.25.-j

Since Bohr-Einstein's photon box thought experiment, storing a photon for a long time has been a dream of physicists. Cavity quantum electrodynamics (CQED) in the microwave domain comes closest to this goal. Photons are trapped in a superconducting cavity and probed by atoms crossing the field one at a time. Experiments with circular Rydberg atoms and Fabry-Perot resonators have led to fundamental tests of quantum theory and various demonstrations of quantum information procedures [1]. The open geometry of the cavity is essential to allow a perturbation-free propagation of long-lived atomic coherences through the mode. With this cavity structure, however, the field energy damping time T_c is very sensitive to geometrical mirror defects, limiting T_c to $\simeq 1$ ms in previous experiments. We report here the realization of a Fabry-Perot resonator at $\omega/2\pi = 51$ GHz, with $T_c = 130$ ms. The cavity quality factor Q is 4.2×10^{10} and its finesse 4.6×10^9 , the highest ever achieved in any frequency domain for this geometry. This important step opens the way to many CQED experiments. Quantum non-demolition detection of a single photon [2] and generation of mesoscopic non-local quantum superpositions [3] are now accessible. Long term storage of single photon fields opens bright perspectives for quantum information processing. These high- Q cavities are also promising for the stabilization of microwave oscillators or for the search of exotic particles [4].

A picture of the cavity C with the top mirror removed is shown in Fig. 1. The mirrors have a diameter $D_0 = 50$ mm. The distance between their apexes is $L = 27.57$ mm. Their surface is toroidal (radii of curvature 39.4 and 40.6 mm in two orthogonal planes). The two TEM_{900} modes near 51.099 GHz with orthogonal linear polarizations are separated by 1.2 MHz. This large frequency splitting is essential to ensure that atoms are efficiently coupled to a single mode only. The mirrors are electrically insulated. A static electric field parallel to the cavity axis is applied between them to preserve

the circular states and to tune the atomic transition via the Stark effect [1]. The 1 cm spacing between mirror edges is partly closed by two guard rings improving the static field homogeneity in C . The atoms of a thermal beam enter and exit the cavity through two large ports (1 cm \times 2 cm) so that they never come close to metallic surfaces, preserving them from patch effect stray fields. This ensures a good transmission of atomic coherences through the cavity [2]. Four piezoelectric actuators are employed to translate one of the mirrors and to tune the cavity (within ± 5 MHz) with a few Hz accuracy.

We realized two mirror sets, M_1 and M_2 . The copper substrates are first machined to a gross spherical shape. They are then submitted to two temperature cycles to release stresses. They are first heated in a vacuum chamber to 400°C and cooled down to liquid N_2 temperature. The final diamond machining is then performed (Kugler company). The local surface roughness is 10 nm r.m.s. and

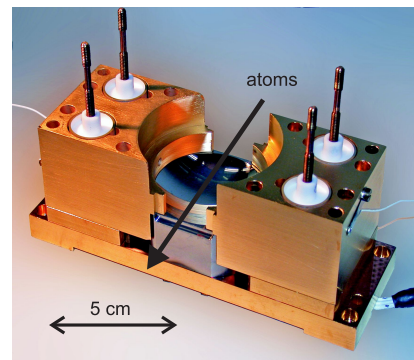


FIG. 1: Photograph of the cavity assembly with the top mirror removed. The atomic beam path is visualized by the arrow. The four posts are used to mount the upper mirror. The piezoelectric actuators, centered by the white Teflon cylinders, surround the posts.

the surface has a peak-to-valley deviation of < 300 nm from the ideal shape. To avoid deformation of the mirrors in the final assembly, their thickness is 30 mm. Their back surface and that of the matching holders are polished to $1 \mu\text{m}$.

The mirror surface is covered with a $12 \mu\text{m}$ -thick layer of Nb. We use a coating facility at CEA, Saclay, designed for r.f. cavities used in particle accelerators [5]. The Nb layer is deposited by d.c. cathode sputtering in a magnetron discharge [6]. We first clean the substrate with ultra-pure filtered alcohol (ultrasonic bath) and dry it with filtered Ar. The sputtering chamber is evacuated to 10^{-8} mbar and then filled with 10^{-1} mbar of Ar. We set the mirror potential to -1000 V for 20 s, creating an Ar plasma which blows away residual dust particles. The chamber is evacuated again and we start the sputtering process. A 1 kW magnetron creates a dense Ar plasma in the vicinity of a cylindrical Nb cathode (Ar pressure during sputtering: 10^{-3} mbar). Initially, the Nb cathode is far away from the mirror. When its impure surface layer is removed, we move it in front of the mirror. The evaporated atoms are deposited at a rate of $0.1 \mu\text{m}/\text{min}$ on the mirror surface, which heats up to $300 - 400^\circ\text{C}$. Before being mounted in the Rydberg atom set-up, the mirrors are finally rinsed in an alcohol ultrasonic bath and dried with Ar.

In order to characterize the cavity modes, microwave is coupled in via weak diffraction loss channels. We thus avoid coupling irises in the mirror centers, which are detrimental to the surface quality [1]. This coupling is large enough to inject a mesoscopic field in C , but not to detect directly the decay of the leaking field. We monitor instead the cavity ring-down with an atomic probe. At the beginning of a measurement sequence, we inject a microwave pulse by a waveguide ending in the guard ring around C . Most of the microwave power is not coupled into the mode and decays in the apparatus in less than $1 \mu\text{s}$. After a time interval t , we send the Rydberg atom probe in C . It is produced by a two-step laser excitation of ^{85}Rb atoms involving a diode laser at 420.30 nm ($5S_{1/2} \rightarrow 6P_{3/2}$) and a second diode laser at 1014.67 nm ($6P_{3/2} \rightarrow 52D_{5/2}$). The cavity field induces transitions from $52D_{5/2}$ to other Rydberg levels. The absorption is made broadband by the Stark effect in a 13.4 V/cm electric field applied in C . Broadband detection is essential for the first cavity tests, since the reproducibility of the mirror mounting results in an uncertainty in the mode frequencies of ± 10 MHz. The cavity-field-induced atomic transitions are monitored by a state-selective field-ionization detector.

By sweeping the microwave source and recording the atomic absorption, we determine the cavity resonances. For M_1 and M_2 we find two modes (lower frequency, M_i^{LF} and higher frequency, M_i^{HF} , $i = 1, 2$) close to 51.1 GHz, separated by the expected 1.2 MHz splitting. We have mapped the transverse profile of these modes. Using pulsed velocity-selected atomic samples, we know the atomic position at any time. Switching the Stark field

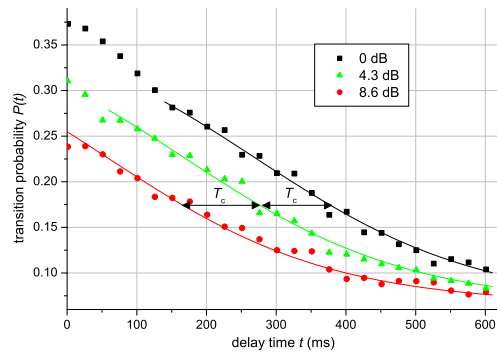


FIG. 2: Measurement of T_c (M_1^{LF}) at $T = 0.8$ K. Transition probability $P(t)$ as a function of the delay t between microwave injection and the atomic probe crossing the cavity. The points (circles, triangles and squares) correspond to three initial field energies E_0 , eE_0 and e^2E_0 , respectively. The fits (solid lines) result from a simple absorption model including saturation. They are equidistantly shifted in time with respect to one another by $T_c = 112 \pm 4$ ms. Each point is the average of 1600 atomic detections.

in C on and off, we set the atoms in resonance during a short time window, at a well defined position in C . The measured transition probability reveals the intensity profile of the mode along the atomic beam axis. We obtain, as expected, a Gaussian with a $w_0 \simeq 6$ mm waist.

To measure the quality factors, we record the transition probability $P(t)$ as a function of the delay t . Typical data, obtained with M_1^{LF} at 0.8 K is shown in Fig. 2 for three initial field energies, E_0 , eE_0 and e^2E_0 (e is the base of natural logarithms), corresponding to microwave source attenuations of 8.6, 4.3 and 0 dB respectively. Due to the exponential decrease of E versus time, $E(t) = E_0 e^{-t/T_c}$, an arbitrary energy $E < E_0$ is reached at times t_0 , $t_0 + T_c$ and $t_0 + 2T_c$ for these three attenuations. Since P depends only upon E , the corresponding $P(t)$ curves are time-shifted by T_c with respect to each other. We obtain $T_c = 112 \pm 4$ ms. For M_1^{HF} , T_c is found to be 87 ± 10 ms. For M_2^{LF} and M_2^{HF} we get, at 0.8 K, $T_c = 74 \pm 6$ ms and $T_c = 130 \pm 4$ ms respectively. These four modes have all an extremely long energy storage time. The longest one corresponds to a light travel distance of 39000 km folded in the 2.7 cm space between the mirrors. The corresponding quality factor is $Q = \omega T_c = 4.2 \times 10^{10}$ and the finesse is $f = Q/9 = 4.6 \times 10^9$.

We have measured the M_2^{HF} mode spectrum at 0.8 K. The FWHM linewidth is 3 ± 0.5 Hz, close to the 1.22 Hz value deduced from T_c . The difference is due to residual low frequency mechanical vibrations (a 1 Hz shift corresponds to a 500 fm translation of one mirror). The cavity drift is less than 3 Hz per hour. The stored field coherence is thus well preserved, an important feature for quantum information storage.

We have studied T_c as a function of the mirror tem-

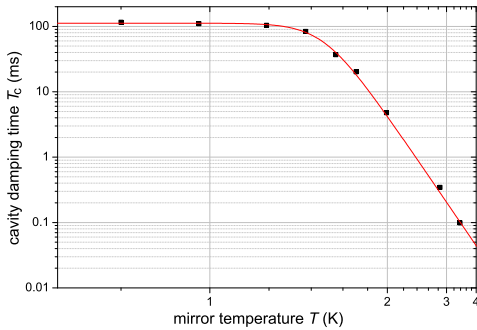


FIG. 3: Cavity damping time T_c versus mirror temperature T (M_1^{LF}). The horizontal scale is reciprocal and the vertical one logarithmic. The dots are experimental. The solid line is a fit providing a gap value $\Delta_0/k_B = 20.2$ K. Below 1.4 K, T_c saturates at 112 ms.

perature T for M_1^{LF} (Fig. 3). For $T > 1.4$ K, T_c increases exponentially versus $1/T$, while it saturates for $T < 1.4$ K. The quality factor Q can be expressed as the ratio G/R_e of two resistances characterizing the geometry ($G = 2800 \Omega$ here) and the losses (R_e) [7]. The effective resistance, $R_e = R_{\text{BCS}} + R_0 + R_d$ has three contributions. The resistance R_{BCS} is given by BCS theory, the residual resistance R_0 at $T = 0$ K is due to defects and R_d measures the diffraction losses. The BCS resistance is $R_{\text{BCS}} = (A/T) \exp(-\Delta_0/k_B T)$, where Δ_0 is the superconducting gap and A is intrinsic to Nb. For $T > 1.6$ K, R_{BCS} dominates R_e , while it is negligible for $T < 1.4$ K. The line in Fig. 3 is a fit with $T_c = G/\omega R_e$, from which we infer $\Delta_0/k_B = 20.2 \pm 0.3$ K. This value, confirmed by measurements on M_1^{HF} and M_2 , differs slightly from the value 17.056 K found at 22 GHz with bulk Nb in Ref. [9].

The saturation of T_c below 1.4 K yields $R_0 + R_d = 75$ n Ω for M_1^{LF} and 68 n Ω for M_2^{HF} . The order of magnitude of the diffraction losses R_d can be estimated. The mirror diameter D_0 limits Q to $Q_{\text{diff}} = (\omega L/c) \exp(D_0^2/2w^2) = 2.7 \times 10^{11}$ ($w = 1.23 w_0$ is the

mode waist at the mirror surface). The surface roughness is characterized by the r.m.s. deviation, h_{rms} , with respect to the ideal shape. The corresponding quality factor, calculated by evaluating the “total integrated scattering” (TIS) [8], is $Q_{\text{surf}} = cL/4\omega h_{\text{rms}}^2$. From the measured $h_{\text{rms}} \simeq 10$ nm, we obtain $Q_{\text{surf}} = 6.4 \times 10^{10}$. Combining these losses yields $Q' = (Q_{\text{diff}}^{-1} + Q_{\text{surf}}^{-1})^{-1} = 5.2 \times 10^{10}$. This is close to the best measured value ($Q = 4.2 \times 10^{10}$), indicating that diffraction losses are the dominant contribution at low T .

It is also instructive to compare the Q factor of our open resonators with that of closed cylindrical cavities at 22 GHz used in Rydberg atom micromaser studies [9, 10]. In these experiments, $Q = 4.0 \times 10^{10}$ at 0.3 K was measured [11]. The residual resistance was $R_0 = G/Q = 28$ n Ω ($G = 1089 \Omega$ – there are no diffraction losses in this geometry), a value comparable to ours. The difference could be due to diffraction losses in our open geometry, to the frequency dependence of R_0 or to variations in the Nb purity. It is remarkable that our open cavity reaches the same Q as the best closed one in the same frequency domain. At much lower frequencies, around 1 GHz, Q factors up to 10^{12} have been obtained [12]. This frequency domain is however much less convenient for cavity QED experiments.

We have reported the realization of a ultra-high- Q photon box. This cavity, with its open geometry, is ideally suited for the propagation of atomic coherence through the field mode, atomic interferometry, decoherence studies and quantum information processing experiments. Experiments with two such cavities are of particular interest. A single atom could be used to entangle two mesoscopic fields separated by a macroscopic distance, resulting in the preparation of a non-local quantum state [3].

Laboratoire Kastler Brossel is a laboratory of Université Pierre et Marie Curie and ENS, associated to CNRS (UMR 8552). We acknowledge support by the Japan Science and Technology Agency (JST), by the EU under the IP projects “QGATES” and “SCALA”, and by a Marie-Curie fellowship of the European Community (S.K.).

-
- [1] J. M. Raimond, M. Brune and S. Haroche, Rev. Mod. Phys. **73**, 565 (2001).
 - [2] S. Gleyzes, S. Kuhr, C. Guerlin, J. Bernu, S. Deléglise, U. Busk Hoff, M. Brune, J. M. Raimond and S. Haroche, Nature (London) in print, quant-ph/0612031.
 - [3] P. Milman, A. Auffeves, F. Yamaguchi, M. Brune, J. M. Raimond and S. Haroche, Eur. Phys. J. D **32**, 233 (2005).
 - [4] R. Bradley, J. Clarke, D. Kinion, L. J. Rosenberg, K. Van Bibber, S. Matsuki, M. Mück and P. Sikivie, Rev. Mod. Phys. **75**, 777 (2003).
 - [5] P. Bosland, A. Aspart, E. Jacques and M. Ribeaudeau, IEEE Trans. Appl. Supercond. **9**, 896 (1999).
 - [6] G. Orlandi, C. Benvenuti, S. Calatroni, M. Hauer and F. Scalaprin, Proceedings of the 6th Workshop on RF Superconductivity **2**, 676 (1993).
 - [7] J. Halbritter, J. Appl. Phys. **42**, 82 (1971).
 - [8] W. Winkler, R. Schilling, K. Danzmann, J. Mizuno, A. Rüdiger and K. A. Strain, Appl. Opt. **33**, 7547 (1994).
 - [9] D. Meschede, H. Walther and G. Müller, Phys. Rev. Lett. **54**, 551 (1985).
 - [10] G. Rempe, F. Schmidt-Kaler and H. Walther, Phys. Rev. Lett. **64**, 2783 (1990).
 - [11] S. Brattke, B. T. H. Varcoe and H. Walther, Phys. Rev. Lett. **86**, 3534 (2001).
 - [12] V. Arbert-Engels, C. Benvenuti, S. Calatroni, P. Darriulat, M. A. Peck, A. M. Valente and C. A. Van't Hof, Nucl. Instrum. Methods A **463**, 1 (2001).